

Cyclodextrin overcomes the transport defect in nearly every organ of NPC1 mice leading to excretion of sequestered cholesterol as bile acid

Benny Liu,* Charina M. Ramirez,[†] Anna M. Miller,[§] Joyce J. Repa,*[§] Stephen D. Turley,* and John M. Dietschy^{1,*}

Departments of Internal Medicine,* Pediatrics,[†] and Physiology,[§] University of Texas Southwestern Medical School, Dallas, TX 75390-9151

Abstract A mutation in NPC1 leads to sequestration of unesterified cholesterol in the late endosomal/lysosomal compartment of every cell culminating in the development of pulmonary, hepatic, and neurodegenerative disease. Acute administration of 2-hydroxypropyl- β -cyclodextrin (CYCLO) rapidly overcomes this transport defect in both the 7-day-old pup and 49-day-old mature *npc1*^{-/-} mouse, even though this compound is cleared from the body and plasma six times faster in the mature mouse than in the neonatal animal. The liberated cholesterol flows into the cytosolic ester pool, suppresses sterol synthesis, down-regulates SREBP2 and its target genes, and reduces expression of macrophage-associated inflammatory genes. These effects are seen in the liver and brain, as well as in peripheral organs like the spleen and kidney. Only the lung appears to be resistant to these effects. Forty-eight h after CYCLO administration to the 49-day-old animals, fecal acidic, but not neutral, sterol output increases, whole-animal cholesterol burden is reduced, and the hepatic and neurological inflammation is ameliorated. However, lifespan is extended only when the CYCLO is administered to the 7-day-old animals. These studies demonstrate that CYCLO administration acutely reverses the cholesterol transport defect seen in the NPC1 mouse at any age, and this reversal allows the sequestered sterol to be excreted from the body as bile acid.—Liu, B., C. M. Ramirez, A. M. Miller, J. J. Repa, S. D. Turley, and J. M. Dietschy. Cyclodextrin overcomes the transport defect in nearly every organ of the newborn or mature NPC1 mouse leading to excretion of the sequestered cholesterol as bile acid. *J. Lipid Res.* 2010. 51: 933–944.

Supplementary key words Niemann-Pick type C • neurodegeneration • liver • lung • lysosome • macrophage • SREBP2 • cholesterol balance • inflammation

This work was supported by U.S. Public Health Service Research Grant RO1 HL09610 (J.M.D., S.D.T.) and by grants from the Moss Heart Fund (J.M.D.) and the Ara Parseghian Medical Research Foundation (J.J.R.). B. L. also received post-doctoral support from the Ara Parseghian Medical Research Foundation and Dana's Angels Research Trust. Its contents are solely the responsibility of the authors and do not necessarily represent the official views of the U.S. Public Health Service or other granting agencies.

Manuscript received 24 July 2009 and in revised form 16 November 2009.

Published, JLR Papers in Press, November 16, 2009

DOI 10.1194/jlr.M000257

Niemann-Pick type C (NPC) disease is one of many lysosomal storage disorders that arise because of inheritance of a mutation inactivating one of the critical enzymes or transporters that operate within the late endosomal/lysosomal (E/L) complex (1). This disorder becomes clinically manifest primarily in children who may present with signs and symptoms of liver or pulmonary disease and/or with various syndromes associated with progressive neurodegeneration (2–4). The molecular defects in NPC disease have been identified as mutations that inactivate either of two proteins, NPC1 (95% of cases) or NPC2 (5% of cases), which normally act in concert to promote the movement of unesterified cholesterol out of the E/L compartment to the cytosolic compartment where it can be metabolized and excreted from the cells (5–9). As a consequence of this transport defect in NPC1 disease, two kinds of pathological alterations are typically found in the organs of humans and mice carrying the *npc1*^{-/-} genotype. First, there is an elevation of the concentration of unesterified cholesterol in the E/L compartment of all cells in the body that increases with age (10, 11). In the central nervous system (CNS) of these individuals, there is also accumulation of GM2 and GM3 gangliosides in neurons (12). Second, this mutation results in macrophage invasion and activation in many tissues like the spleen, liver, and lung, as well as activation of glial cells within the CNS (1, 13). These activated monocyte-derived cells synthesize and release many pro-inflammatory proteins into each of these organs (14, 15). Presumably, it is the combined effect of these two different pathological lesions that ultimately leads to parenchymal cell death and clinical disease.

Abbreviations: BBB, blood brain barrier; CNS, central nervous system; CYCLO, 2-hydroxypropyl- β -cyclodextrin; E/L, late endosomal/lysosomal; ER, endoplasmic reticulum; LDLR, low density lipoprotein receptor; LXR, liver X receptor; NPC, Niemann-Pick type C; SREBP, sterol regulatory element-binding protein.

¹To whom correspondence should be addressed.

e-mail: john.dietschy@utsouthwestern.edu

The cholesterol that becomes sequestered in the E/L compartment of cells in NPC1 disease comes from several sources, depending upon the tissue. Many organs utilize the low density lipoprotein receptor (LDLR) to take up lipoproteins carrying either apoB₁₀₀ or apoE through receptor-mediated endocytosis (16). This process is particularly important in liver and adrenal gland which have high levels of LDLR activity (17). Other organs like the spleen and lung rely more on bulk-phase endocytosis for lipoprotein uptake (13). Unlike all other organs, the cells of the CNS do not have access to plasma lipoproteins (18, 19) but take up unesterified cholesterol complexed to apoE that has been synthesized in astrocytes (20–22). Regardless of the source, this sterol becomes sequestered in the E/L compartment of all of these different cells. In general, the severity of organ damage is proportional to the amount of cholesterol reaching the cells. Thus, the level of disease in a particular tissue is made worse when more cholesterol is forced into an organ through either receptor-mediated or bulk-phase endocytosis (13, 23), whereas the disorder is ameliorated when the uptake of lipoprotein- or apoE-associated cholesterol is reduced (23, 24).

An alternative approach to reversing NPC1 disease recently came from the observation that administration of the cholesterol-binding agent, 2-hydroxypropyl- β -cyclodextrin (CYCLO), to the NPC1 mouse significantly improved the liver and CNS disease and prolonged life (25–27). Because this agent is known to extract cholesterol from the plasma membrane of cells in vitro (28, 29), it was assumed that this molecule might somehow extract the sequestered cholesterol from the E/L compartment of cells in vivo and carry it to the kidney for excretion in the urine (30). However, no known pathway exists for rapidly moving sequestered lysosomal sterol to the plasma membrane, and further, recent observations strongly suggested that after CYCLO administration, the unesterified cholesterol moved rapidly into the cytosolic compartment for processing. Twenty-four h after administration of CYCLO, there was a decrease in the concentration of unesterified cholesterol in cells throughout the body, an increased concentration of cholesteryl esters, an increase in the relative mRNA levels for liver X receptor (LXR) regulated target genes, and inhibition of sterol regulatory element binding protein (SREBP) and its target genes (27). Apparently CYCLO had overcome the transport defect brought about by the NPC1 mutation and allowed the unesterified cholesterol in the E/L compartment to reach the cytosol for esterification by ACAT, the nucleus to activate the LXR system (31, 32) and the endoplasmic reticulum (ER) to suppress the SREBP sterol-sensing apparatus (33, 34).

This observation that CYCLO acutely overcame the transport defect was particularly important as it not only identified a potential therapy that might be useful in reversing the NPC1 defect, but it also provided a possible approach to better understanding the molecular events whereby NPC1 and NPC2 interact to promote unesterified cholesterol movement from the E/L complex to the cytosolic compartment. The current studies were designed to further explore this important observation and to obtain

new information in four specific areas. First, while the reported studies were carried out only in very young mice (27), it was essential to determine how the age of the animals affected the plasma level and excretion rate of the CYCLO molecule. Second, it was also critical to determine if age had any effect on the ability of CYCLO to reverse the transport defect in the *npc1*^{−/−} mice. This was particularly important with respect to correction of the transport defect in the CNS where permeability of the blood brain barrier (BBB) might change with aging. Third, following CYCLO administration, the total body burden of cholesterol was known to be reduced, so studies were undertaken to identify which pathway was utilized to excrete this sequestered cholesterol from the treated mice. Fourth, while CYCLO administration corrected the biochemical defect in many tissues at any age, it was important to establish whether the age of the mice at the time of treatment ultimately affected the lifespan of the mutant animals. Together, these studies provide new information on several important aspects of the correction of the transport defect in NPC disease by CYCLO.

MATERIALS AND METHODS

Animals

Control (*npc1*^{+/+}) and homozygous mutant (*npc1*^{−/−}) mice were generated from heterozygous (*npc1*^{+/-}) animals with a pure BALB/c background (7, 26). Most pups were genotyped at 19 days of age except in those experiments utilizing 7-day-old animals where the pups were genotyped at 5 days of age. All animals were housed in plastic colony cages in rooms with alternating 12 h periods of dark and light, and were studied in the fed state at the end of the dark phase. For the experiments using 49-day-old mice, with one exception, there were comparable numbers of males and females in each group. In the experiment measuring fecal neutral and acidic sterols, only male mice were used. All experimental protocols were approved by the Institutional Animal Care and Use Committee of the University of Texas Southwestern Medical School.

Treatment and diets

All animals except the heterozygous breeding stock were fed ad libitum a cereal-based, low-cholesterol (0.02% w/w) diet (no. 7001; Harland Teklad, Madison, WI) upon weaning at 19 days of age. The breeding stock was maintained on a different formulation with a higher fat content (No. 7002; Harlan Teklad, Madison, WI). Mice were administered a single subcutaneous injection during the late dark phase (09:00 h) at the scruff of the neck at either 7 or 49 days of age, of a 20% (w/v, in saline) solution of 2-hydroxypropyl- β -cyclodextrin (4000 mg/kg body weight) (Sigma; product H107) (26, 27). Matching mice injected with saline alone served as controls.

CYCLO pharmacokinetics and plasma concentrations

Whole-body CYCLO clearance was measured in 7- and 49-day-old *npc1*^{+/+} and *npc1*^{−/−} mice using ¹⁴C-labeled 2-hydroxypropyl- β -cyclodextrin with an average degree of substitution of 5.15 and a specific activity of 6.95 mCi/g (Cyclodextrin Technologies Development, Inc, High Springs, FL). The stock [¹⁴C]CYCLO solution contained 1.0 mCi in 1.0 mL of water. Aliquots of the stock solution were added to a 20% (w/v) solution of non-radio-labeled CYCLO giving approximately 40,000 cpm/ μ L that was

used in the 7-day-old mice, or 10,000 cpm/ μ L that was used in the 49-day-old mice. At each time point 2–4 animals were studied. The mice were given a subcutaneous injection of the [14 C]CYCLO solution (4000 mg/kg) at the scruff of the neck and then studied at various time points. Some mice were terminated immediately upon completion of the injections. Such animals served as “zero time” controls. The other mice that were killed later were returned to their cages following administration of the [14 C]CYCLO. At the time of study, the mice were euthanized, rinsed with ethanol to remove contaminating [14 C]CYCLO on the skin and fur, and saponified in alcoholic KOH. The carcasses were digested on a steam bath, transferred into 100 mL flasks, and the volume brought to 100 mL with ethanol. Duplicate 1.0 mL aliquots of the liquefied carcass were transferred into glass counting vials to which was added 15 mL of Cytosint (MP Biomedicals, Irvine, CA). The total body counts, normalized to body weight, recovered from animals terminated at each time point and were expressed as a percentage of the normalized counts that were present in the tissues of the “zero time” control animals. These percentage recoveries were used to calculate the proportion of the administered dose of [14 C]CYCLO that had been cleared from the animal over each time interval. These data were taken as a measure of the “whole-animal” turnover rate of CYCLO in the 7- and 49-day-old mice.

Plasma CYCLO concentrations were also determined in 7- and 49-day-old mice. Aliquots of the stock solution of [14 C]CYCLO were added to the 20% (w/v) solution of non-radio-labeled CYCLO giving approximately 400,000 cpm/ μ L, which was used in the 7-day-old mice, and 10,000 cpm/ μ L, which was used in the 49-day-old mice. The mice were administered a subcutaneous injection of CYCLO at the scruff of the neck and then studied at various time points. At the time of study, the mice were euthanized, and blood was collected from the inferior vena cava of each animal and placed in centrifuge tubes. In the 7-day-old mice, 15–30 μ L of plasma was collected, and in the 49-day-old mice, 100 μ L of plasma was collected. The plasma was then transferred into glass counting vials containing 15 mL of Cytosint and counted. From the stock solution specific activity, plasma CYCLO concentrations were determined and were expressed as the mg of CYCLO per mL of plasma.

Tissue cholesterol concentrations and synthesis rates

Both the 7- and 49-day-old mice were studied 24 h after the injection of CYCLO. At the time of study they were exsanguinated. In 7-day-old mice, the liver, brain, and remaining carcass were collected; in 49-day-old mice, the liver, brain, adrenal, spleen, kidney, lung, and remaining carcass were harvested. These tissues were saponified in alcoholic KOH and the cholesterol was extracted and quantitated by gas chromatography using stigmasterol as the internal standard (35). The tissue cholesterol levels were expressed as either mg of cholesterol per g wet weight of tissue (mg/g) or mg of cholesterol per whole organ (mg/tissue). The total cholesterol values found in every tissue were summed to give whole-animal cholesterol contents, and these values were expressed as mg of cholesterol per kg body weight (mg/kg). The rates of cholesterol synthesis in all of the tissues were measured in vivo as previously described (35). Each animal was administered a bolus of [3 H]water and studied 1 h later. These rates were expressed as the amount of [3 H]water incorporated into sterols per h per g wet weight of tissue (nmol/h/g). The [3 H]water incorporation rates in all organs were summed and used to calculate the whole-animal synthesis rates. These rates were then converted to the absolute mg of cholesterol synthesized each day per kg body weight (mg/day/kg) (36, 37). Unesterified and esterified cholesterol levels in tissues were measured as previously described (23) and were expressed as the mg of unesterified or esterified cholesterol per g wet weight of tissue (mg/g).

Relative mRNA levels

The liver and brain of each animal were collected, snap-frozen in liquid nitrogen, and stored at -85°C . Total RNA was isolated from these tissues using RNA STAT-60 (Tel-Test, Inc.). RNA concentrations were determined by absorbance at 260 nm with a Thermo Scientific Nanodrop 100 Spectrophotometer. The total RNA was treated with RNase-free DNase (Roche) and reverse-transcribed into cDNA with SuperScript II reagents (Invitrogen) as previously described (38). Quantitative real-time PCR was performed using an Applied Biosystems 7900HT sequence detection system and SYBR-green chemistry (39). The nucleotide sequences of the various primers used were published (15, 27). The mRNA levels are expressed relative to the housekeeping gene, cyclophilin, calculated by the comparative C_T method (40) and mathematically adjusted to express the controls in each age group with a unit of 1.0.

Liver function test

Plasma was sent to a commercial laboratory for measurements of the liver function test, alanine aminotransferase (ALT).

Fecal neutral sterol and bile acid excretion

All mice were individually housed for performing stool collections. Prior to initiation of the stool collections, the mice were acclimated to individual housing conditions for a period of at least 5 days. A 3-day baseline stool collection was then performed for each animal between 46–48 days of age. At 49 days of age, the mice were administered either a 20% (w/v) solution of CYCLO or saline alone subcutaneously at the scruff of the neck. Stool from each animal was then collected every 24 h for a total of 6 days after the CYCLO injection. Fecal neutral and acidic sterol excretion was measured as previously described (35). These values were expressed as the mg of sterol excreted per day per kg body weight (mg/day/kg).

Survival studies

The general clinical condition of the mice was monitored daily. Once the animals began to show difficulty accessing the pelleted diet, they were provided access to a powdered form of the diet. When mice were no longer able to take in food or water, they were euthanized, and this was considered the day of death.

Data analysis

All data are presented as the mean \pm SEM. Differences between these mean values were tested for statistical significance ($P < 0.05$) using one-way ANOVA, followed by the Newman-Keuls multiple comparison test (Graph-Pad Software, Inc., San Diego, CA). Significant differences between groups are designated with different letters. Statistical differences among survival curves were determined utilizing the Wilcoxon-Gehard and log-rank analyses.

RESULTS

Before exploring the specific effects of CYCLO in newborn and mature mice with the NPC1 mutation, it was first necessary to define how the parameters of disordered cholesterol physiology changed with animal age and, second, to establish if the pharmacokinetics of CYCLO varied in the young and mature animals.

Natural history of the *npc1*^{-/-} mouse

While previous publications have described some of the changes in sterol metabolism seen with aging of *npc1*^{-/-} animals (10, 11), it was important to better define these

baseline changes before exploring the effects of CYCLO. As seen in **Fig. 1**, the hallmark of the NPC1 mutation is accumulation of cholesterol in nearly all tissues of the body. As the liver is responsible for the uptake of most plasma lipoproteins, it bears the brunt of this mutation. While hepatic cholesterol content only increased from 0.6 mg at birth to 3.2 mg at 49 days of age in the *npc1*^{+/-} mice, changes that reflected in the growth of this organ, there

was progressive accumulation of cholesterol in the liver of the *npc1*^{-/-} mice with the cholesterol content reaching nearly 30 mg (A). This change was due to both the accumulation of sterol within individual cells as well as to an increase in relative liver size from 5.8% of body weight to 8.5%. Accumulation of cholesterol in the remaining organs of the carcass was less dramatic since these tissues take up smaller amounts of lipoprotein cholesterol than

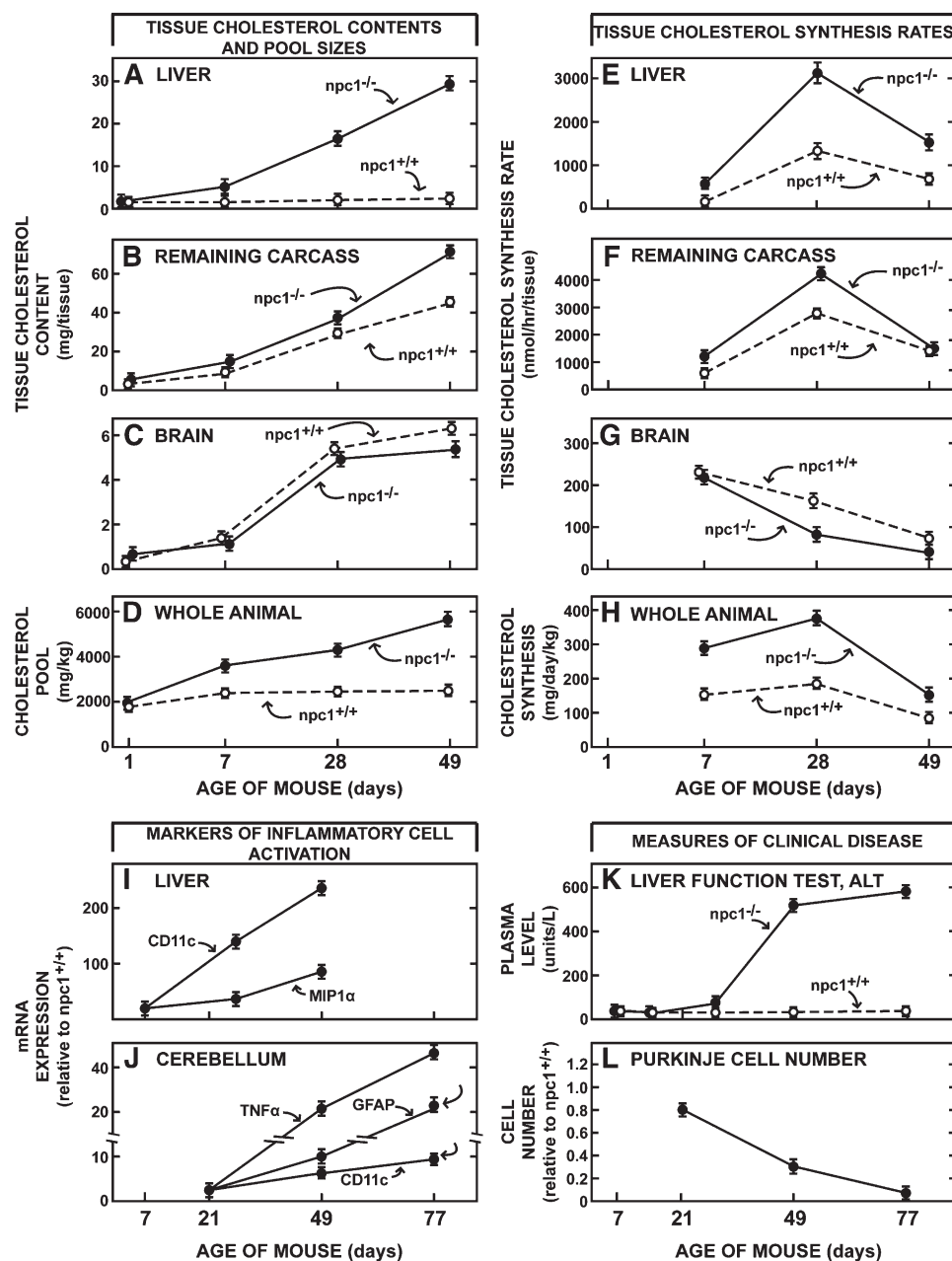


Fig. 1. Natural history of the changes in sterol metabolism and clinical findings in *npc1*^{+/-} and *npc1*^{-/-} mice as a function of age. The first set of panels illustrate the changes in cholesterol content of the liver (A), carcass (B), brain (C) and whole animal (D) at different ages, and the second set shows the rates of cholesterol synthesis measured in vivo in these same tissues (E–H). The data in panels D and H are normalized to a whole-animal weight of 1 kg. The changes in relative mRNA levels of various macrophage-associated proteins in the liver (I) and cerebellum (J) are also shown as a function of age as is the liver function test ALT (K) and relative Purkinje cell number in the cerebellum (L). These various curves were constructed from data obtained in the current study as well as in previously reported investigations. Each value represents the mean ± 1 SEM for 4–8 animals at each age. NPC, Niemann-Pick type C.

the liver (Fig. 1B). The brain is the one tissue that behaved differently. The cholesterol content of this organ in the *npc1*^{+/+} mice increased from 0.2 mg to 6.1 mg over 49 days, whereas, in the *npc1*^{-/-} animals, this increase in content was slightly less (Fig. 1C). Even though cholesterol also accumulates in the glia and neurons of the brain (11, 12), this small decline in content reflected both early demyelination and a small reduction in brain weight. As a result of all of these changes, the whole-animal cholesterol pool progressively rose to nearly 5,800 mg/kg in the *npc1*^{-/-} mice, while it remained essentially constant at about 2,300 mg/kg in the *npc1*^{+/+} animals over these 7 weeks of life (Fig. 1D). The rates of cholesterol synthesis also varied markedly with age. Because of the perceived shortage of sterol in the cytosolic compartment of all cells, rates of cholesterol synthesis were higher at every age in the *npc1*^{-/-} mice compared with the control animals (Fig. 1E, F). Again, the brain was the exception as synthesis tended to be slightly reduced in this organ in the older mutant mice (Fig. 1G). Nevertheless, overall, by 49 days of age when the cholesterol pool in the *npc1*^{-/-} mice had expanded 2.6-fold, the rate of whole-animal synthesis was still nearly double that seen in the *npc1*^{+/+} animals (Fig. 1H).

Associated with these changes in cholesterol metabolism were age-dependent changes in the molecular markers of macrophage infiltration and activation, and the appearance of clinical disease. In the liver, for example, there was a progressive rise of the mRNA levels of CD11c and MIP-1 α (Fig. 1I) and in the cerebellum, of the inflammatory markers TNF α , GFAP, and CD11c as the *npc1*^{-/-} animals aged (Fig. 1J). At the same time, the liver function test ALT abruptly increased, particularly after 28 days of age (Fig. 1K), and there was progressive loss of Purkinje cells in the cerebellum (Fig. 1L). Thus, it was clear from these preliminary investigations that the baseline values for all of these parameters of cholesterol metabolism, macrophage infiltration, and clinical disease were very different in the young, 7-day-old and mature, 49-day-old *npc1*^{-/-} mice.

Pharmacokinetics of CYCLO in young and mature mice

Since CYCLO is known to be cleared from the plasma almost entirely by the kidneys (41), it was next important to determine if maturation of renal function significantly altered the time this molecule would be in the plasma and, thus, accessible to the tissues of the body. As shown in Fig. 2, there were marked differences in the rates of clearance of CYCLO in the 7-day-old and 49-day-old mice. At a dose of 4,000 mg/kg, only about 40% of the CYCLO had been cleared from the body of the 7-day-old mice 6 h after the subcutaneous injection, while more than 90% had been removed in the 49-day-old animals (Fig. 2A). These marked differences in whole-body clearance were reflected in the concentration CYCLO achieved in the plasma. Following administration of the compound to the 49-day-old mice, the plasma concentration of CYCLO reached only 1.87 mg/mL (1.34 mM) within 0.5 h of administration and then rapidly fell to near 0 by 3 h (Fig. 2B). In contrast, in the immature, 7-day-old mice, the concentration reached values nearly three times higher (5.12 mg/mL, 3.67 mM)

and these remained high for nearly 6 h. Of note, these findings were identical in both the *npc1*^{+/+} and *npc1*^{-/-} animals. From the areas under these two curves it could be calculated that in animals given the same 4,000 mg/kg dose, the exposure time of the cells of the body to CYCLO in the plasma was 6 times greater in the 7-day-old mice than in the mature animals. Thus, it could be anticipated that the metabolic effects of this dose of CYCLO might be very different in these two groups of animals. In a parallel group of mice, the rate of cholesterol excretion in the urine after administration of the CYCLO was also quantitated. While nearly all of the [¹⁴C]CYCLO was recovered in the urine, the total output of cholesterol was less than 1.0 mg/day/kg (less than 0.5% of the sterol excreted in the feces during this 24 h period).

Effects of CYCLO in the liver of the *npc1*^{-/-} mice

As the liver exhibits the most profound abnormalities in cholesterol metabolism in the *npc1*^{-/-} mice and as the reflection coefficient for CYCLO in the liver sinusoids is likely to be zero, the effect of this compound on the hepatocytes and macrophages of this organ was next explored. As seen in Fig. 3, the concentration of unesterified cholesterol was markedly elevated (Fig. 3A, B) while the concentration of cholesteryl esters was lower (Fig. 3C, D) in the *npc1*^{-/-} mice that were either 7 or 49 days of age, compared with the control mice. Twenty-four h after treatment with CYCLO there was a similar decrease in the concentration of unesterified cholesterol in these two groups (Fig. 3A, B), and there was a similar, marked increase in the concentration of cholesteryl esters (Fig. 3C, D). The rates of cholesterol synthesis were significantly higher in the 49-day-old *npc1*^{+/+} mice than in the younger control animals (Fig. 3E, F) so that the relative increase seen in synthesis was greater in the 7-day-old *npc1*^{-/-} mutants than in the 49-day-old animals (Fig. 3E, F). Nevertheless, treatment with CYCLO suppressed the rate of cholesterol synthesis in both age groups to nearly zero. Of interest, these same effects were seen regardless of whether the CYCLO was prepared and administered in plastic or glass containers. Also of importance, CYCLO administration had no effect on either the concentration of unesterified or esterified cholesterol (Fig. 3A–D) or on the rate of cholesterol synthesis (Fig. 3E, F) in the *npc1*^{+/+} mice of either age.

While these findings indicated that 24 h after CYCLO administration, sterol from the sequestered pool had moved to the cytosolic compartment and been esterified, a portion of this unesterified cholesterol also had interdigitated into the ER and affected expression of SREBP2 and its target genes (33, 34). The relative mRNA levels of the genes for SREBP2, HMG-CoA SYN, and LDLR tended to be elevated in the untreated, *npc1*^{-/-} mice of both ages (Fig. 3G–L), presumably reflecting the low levels of cholesterol in the cytosolic compartment of these mutant mice. Following CYCLO treatment, however, these mRNA levels were all markedly suppressed. Finally, the mRNA levels of the macrophage markers CD11c (Itgax), CD68 (macrosialin), and MIP-1 α (Ccl3) were markedly elevated in the 49-day-old, but not the 7-day-old, *npc1*^{-/-} mice (Fig. 3M–R).

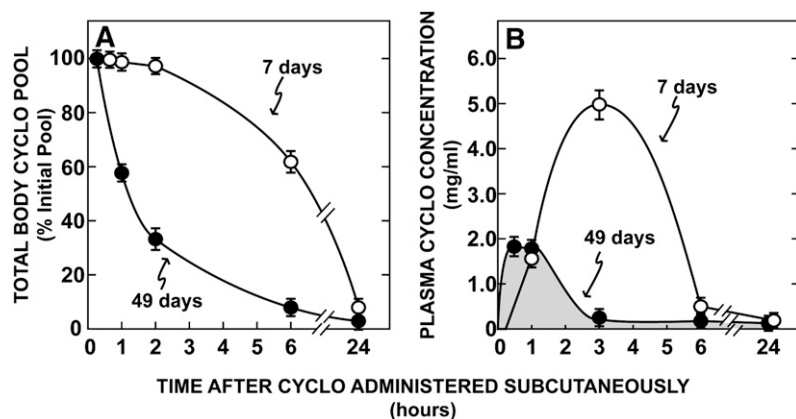


Fig. 2. Time course for the clearance of CYCLO from the whole animal (A) and plasma (B). These data were determined in 7- and 49-day-old *npc1*^{+/+} and *npc1*^{-/-} mice injected at time 0 with a subcutaneous bolus of CYCLO (4,000 mg/kg) also containing [¹⁴C]CYCLO. Groups of animals were then killed 0, 0.5, 1, 2, 3, 6, and 24 h after the injection, and the total body pool and plasma concentration of CYCLO were determined. As data from the two genotypes were the same, they have been combined in this figure. Each data point represents the mean \pm SEM for 4–6 animals in each group. CYCLO, 2-hydroxypropyl- β -cyclodextrin.

Twenty-four h after administration of CYCLO, these levels of expression were all suppressed. Surprisingly, even the very abnormal liver function test ALT was nearly normalized by this treatment (Fig. 3T).

Effects of CYCLO in the brain of the *npc1*^{-/-} mice

Of particular importance was whether CYCLO could reach the brain equally well in the young and old animals given the findings that the concentration this compound achieved in the plasma was much less (Fig. 2) and the reflection coefficient for the molecule likely approached 1.0 in the 49-day-old *npc1*^{-/-} mouse brain. As is evident in Fig. 4, the baseline findings in the brain were very different in the young and old mice. The concentration of unesterified cholesterol increased markedly from approximately 4 mg/g in the 7-day-old *npc1*^{+/+} animals to nearly 15 mg/g in the mature control mice as the brain became fully myelinated (Fig. 4A, B). The level of cholesteryl esters was extremely low (Fig. 4C, D), compared with the liver, and there was a marked decline in the rate of sterol synthesis as the CNS reached maturity (Fig. 4E, F). In the untreated *npc1*^{-/-} animals, in contrast to the liver, there were relatively small differences found in these three parameters of sterol metabolism, although as previously reported (24), there was a trend for the concentration of unesterified cholesterol and the rate of synthesis to be slightly lower in the brain of the 49-day-old mutant animals. This presumably reflected both the mild demyelination and neuron loss known to be present in these older animals. Following CYCLO administration there was little change in the concentration of unesterified cholesterol in either age group (Fig. 4A, B), but there was a significant increase in the level of cholesteryl esters (Fig. 4C, D) and suppression of synthesis (Fig. 4E, F) in both the 7- and 49-day-old *npc1*^{-/-} mice. Similarly, the relative mRNA levels of SREBP2 (Fig. 4G, H), HMG-CoA SYN (Fig. 4I, J), and CD11c (Fig. 4K, L) were all significantly lower following CYCLO administration, and the relative level of this suppression was approximately the same in both age groups.

Effects of CYCLO in the other extrahepatic organs of the *npc1*^{-/-} mice

Not only did CYCLO reverse the transport defect in the liver and brain, but as seen in Fig. 5, it also significantly

altered cholesterol metabolism in the other major organs. In the 49-day-old *npc1*^{-/-} animals, the concentration of unesterified cholesterol (Fig. 5A–D, G, J) and the rates of cholesterol synthesis (Fig. 5C, F, I, L) were elevated in tissues like the adrenal, spleen, kidney, and lung. Twenty-four h after CYCLO administration, the adrenal, spleen, and kidney responded with a reduction in the concentration of unesterified cholesterol, an increase in cholesteryl esters (Fig. 5B, E, H), and marked suppression of sterol synthesis (Fig. 5C, F, I). Of importance, the lung was relatively unresponsive in that there was no significant change in the level of unesterified cholesterol (Fig. 5J) and no suppression of cholesterol synthesis (Fig. 5L), even though a small increase in the concentration of cholesteryl esters occurred (Fig. 5K). Conceivably, this different response may have reflected intra-alveolar macrophages that did not have access to plasma CYCLO.

Effect of CYCLO on whole-animal cholesterol metabolism

These effects of CYCLO seen in individual organs should reflect major shifts in whole-animal cholesterol metabolism. This was found to be the case, as illustrated in Fig. 6. The whole-animal cholesterol pool was essentially the same in 7-day-old *npc1*^{+/+} mice (2,347 mg/kg) (Fig. 6A) and in 49-day-old animals (2,410 mg/kg) (Fig. 6B), even though whole-animal cholesterol synthesis was twice as high (150 mg/day/kg) in the young mice (Fig. 6C) as in the mature animals (84 mg/day/kg) (Fig. 6D). This reflected the need for plasma membrane cholesterol in the rapidly growing, 7-day-old mice. Importantly, CYCLO administration to these control animals did not alter either parameter of whole-body cholesterol metabolism. Whole-animal cholesterol synthesis rates were significantly increased in both the 7-day-old (296 mg/day/kg) (Fig. 6C) and 49-day-old (124 mg/day/kg) (Fig. 6D) *npc1*^{-/-} animals, as were the cholesterol pools (Fig. 6A, B). Within 24 h, administration of CYCLO reduced the whole-animal cholesterol pool in the 7-day-old mice by 469 mg/kg (Fig. 6A) but by only 105 mg/kg (Fig. 6B) in the older animals. Nevertheless, in both instances, whole-animal cholesterol synthesis was markedly suppressed (Fig. 6C, D). Thus, the acute effects of CYCLO seen in the individual organs had caused significant changes in whole-animal cholesterol metabolism within just 24 h.

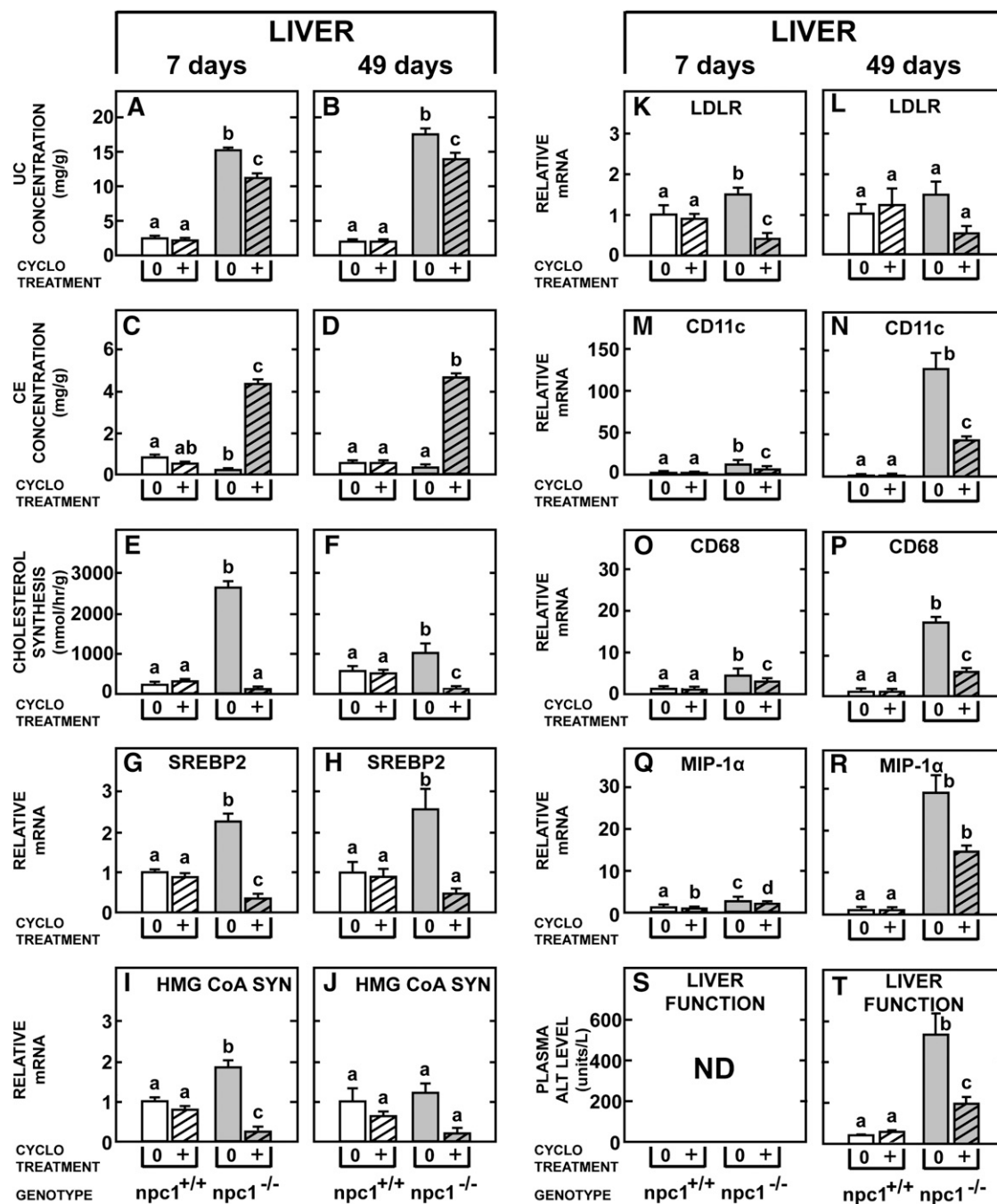


Fig. 3. Comparison of the acute effects of CYCLO in the liver of 7- and 49-day-old *npc1*^{+/+} and *npc1*^{-/-} mice. Each animal was given a single, subcutaneous dose of CYCLO (4,000 mg/kg) and studied 24 h later. The concentrations of hepatic unesterified cholesterol (A, B) and cholesteryl esters (C, D), as well as rates of cholesterol synthesis (E–F) were determined. The relative mRNA levels of SREBP2 and its target genes (G–L) and various macrophage-associated proteins (M–R) were also measured. The liver function test ALT was quantitated in the 49-day-old (T), but not in the 7-day-old (S) animals. Each column represents the mean \pm SEM for 6 animals in each group. Significant differences among groups are designated by different letters in each panel. CE, cholesteryl ester; CYCLO, 2-hydroxypropyl- β -cyclodextrin; LDLR, low density lipoprotein receptor; ND, not determined; NPC, Niemann-Pick type C; SREBP, sterol regulatory element-binding protein; UC, unesterified cholesterol.

Effect of CYCLO on fecal sterol excretion

If CYCLO administration to the *npc1*^{-/-} mice reversed the block in cholesterol transport and allowed the sequestered unesterified sterol to be metabolized normally in the cytosolic compartment of cells, then this cholesterol ultimately must be excreted from the body either as fecal neutral sterols or after conversion to bile acid, as fecal acidic

sterols. To explore this possibility, detailed external sterol balance studies were undertaken in these four groups of 49-day-old mice. As shown in **Fig. 7**, in *npc1*^{+/+} animals 46–48 days of age, the basal rate of total fecal sterol excretion equaled 126 mg/day/kg, 69 mg of which was as neutral sterols (Fig. 7A) while 57 mg was as acidic sterols (Fig. 7B). As has been previously reported (42) in the *npc1*^{-/-} mice,

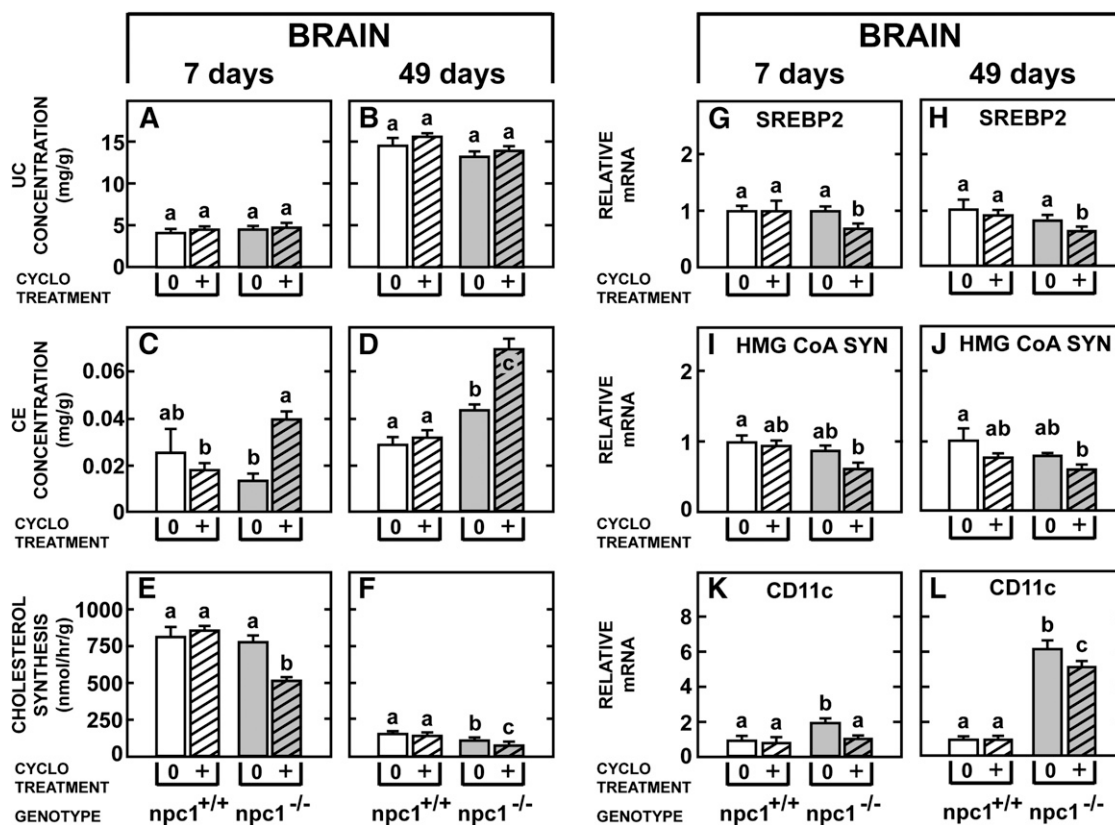


Fig. 4. Comparison of the acute effects of CYCLO in the brain of 7- and 49-day-old *npc1*^{+/+} and *npc1*^{-/-} mice. Each animal was given a single, subcutaneous dose of CYCLO (4,000 mg/kg) and studied 24 h later. The concentrations of unesterified cholesterol (A, B) and cholesteryl esters (C, D), as well as rates of cholesterol synthesis (E–F) in the whole brain were determined. The relative mRNA levels of SREBP2 (G–H), HMG-CoA SYN (I, J), and the inflammatory protein CD11c (K, L) were also quantified. Each column represents the mean \pm SEM for 6 animals in each group. Significant differences among groups are designated by different letters in each panel. CE, cholesteryl ester; CYCLO, 2-hydroxypropyl- β -cyclodextrin; NPC, Niemann-Pick type C; SREBP, sterol regulatory element-binding protein; UC, unesterified cholesterol.

basal total sterol excretion was higher (199 mg/day/kg), principally because the excretion of neutral sterols (134 mg/day/kg) was elevated (Fig. 7C) while acidic sterol output (65 mg/day/kg) was about the same (Fig. 7D) as seen in the *npc1*^{+/+} mice. Very importantly, administration of CYCLO to the *npc1*^{+/+} animals lacking the sequestered pool of unesterified cholesterol in the E/L compartment had no effect on fecal sterol output (Fig. 7A, B). In contrast, 48 h after CYCLO administration to the *npc1*^{-/-} mice, fecal acidic sterol excretion had increased to over 100 mg/day/kg (Fig. 7D) before returning to normal values six days after administration of the CYCLO. The excretion of neutral sterols, however, was unaffected by this treatment (Fig. 7C). From these data it could be calculated that the administration of CYCLO to the *npc1*^{-/-} mice increased total sterol output by approximately 150 mg/kg over this six-day period.

Effect of age at treatment on prolongation of life

Finally, while all of these studies indicated that CYCLO did reverse the transport defect in NPC1 disease and led to a reduction in whole-animal cholesterol burden, the overall effect of these favorable changes on animal longevity had to be examined. As shown in Fig. 8, control *npc1*^{-/-} mice treated with only saline spontaneously died between 80 and

100 days of age with a median life span of 88 days. In those animals given CYCLO at 7 days of age, median survival was significantly increased to 118 days, while those mice treated at 49 days of age had no significant benefit. Thus, while the transport defect could be reversed in the older animals, these mice already had severe tissue damage (Fig. 1) that could not be rescued by CYCLO administration.

DISCUSSION

These studies provide new information on the characteristics of the process whereby administration of the cholesterol-binding agent CYCLO reverses the lysosomal transport defect found in NPC1 disease. Even though the mature, 49-day-old animals cleared CYCLO from the blood more quickly than the 7-day-old mice (Fig. 2), both groups of animals responded well to this treatment, with signals that the sequestered unesterified cholesterol from the E/L compartment had flowed into the cytosolic compartment of cells in most tissues. There was an increase in the concentration of cholesteryl esters and suppression of sterol synthesis and SREBP2 target genes in most organs, including the CNS (Figs. 3–5). In both the 7-day-old and 49-day-old *npc1*^{-/-} mice, this treatment resulted in a reduction of

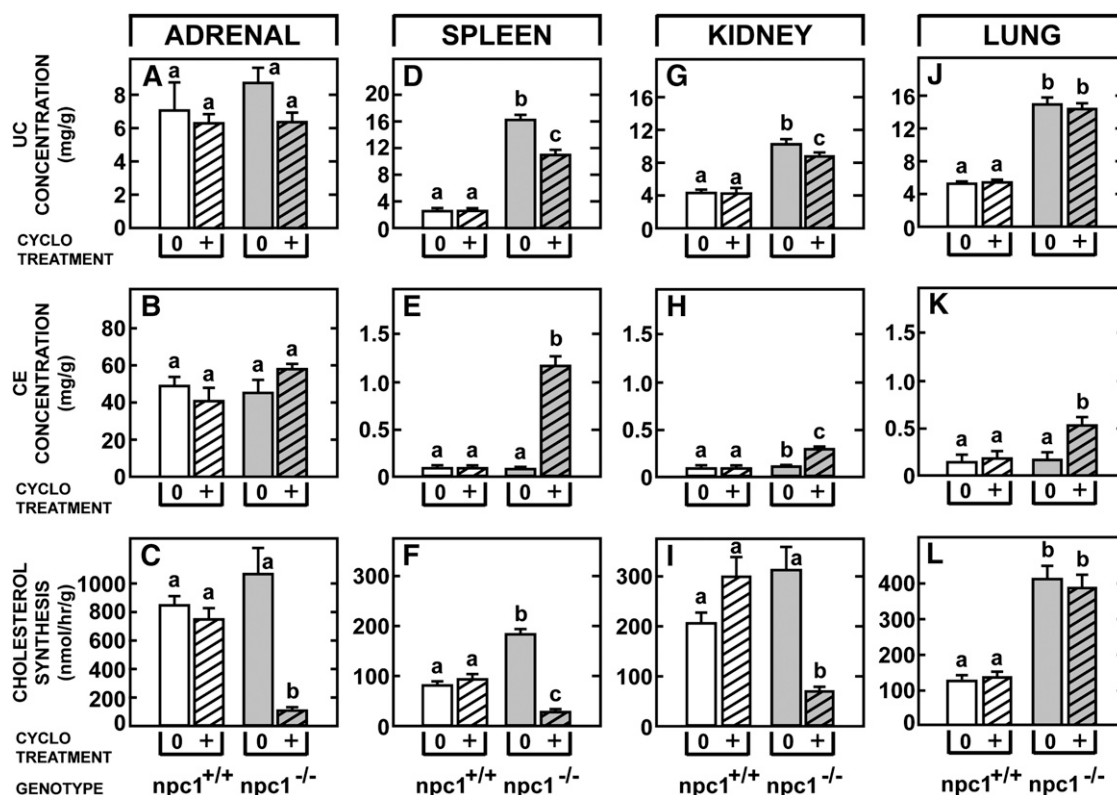


Fig. 5. Comparison of the acute effects of CYCLO in the adrenal gland, spleen, kidney, and lung 49-day-old $npc1^{+/+}$ and $npc1^{-/-}$ mice. Each animal was given a single, subcutaneous dose of CYCLO (4,000 mg/kg) and studied 24 h later. The concentration of unesterified cholesterol (A, D, G, J) and cholesteryl esters (B, E, H, K), as well as rates of cholesterol synthesis (C, F, I, L) were measured in each of these organs. Each column represents the mean \pm SEM for 6 animals in each group. Significant differences among groups are designated by different letters in each panel. CE, cholesteryl ester; CYCLO, 2-hydroxypropyl- β -cyclodextrin; NPC, Niemann-Pick type C; UC, unesterified cholesterol.

whole-body cholesterol burden (Fig. 6) (27) that, in the older animals, was brought about by fecal excretion of excessive amounts of bile acid (Fig. 7). When this acute reduction in cellular cholesterol content was carried out in young 7-day-old animals before there was severe tissue damage, lifespan was significantly prolonged (Fig. 8).

In addition to these general features, however, these studies provide important quantitative information on five aspects of this process whereby CYCLO overcame the defect in intracellular cholesterol transport caused by the mutation in NPC1. First, these studies support the concept that in vivo CYCLO works by enhancing cholesterol transport out of the lysosome and not by extracting sterol from plasma membranes, as it does in cells studied in culture (28, 29). Administration of this compound to $npc1^{+/+}$ animals did not increase the rate of cholesterol synthesis, activate SREBP2 target genes, or alter fecal sterol excretion (Figs. 3, 5, 7). Only when sequestered pools of unesterified cholesterol were present, as in the cells of the $npc1^{-/-}$ animals, did treatment with CYCLO release the excess sterol to flow into the cytosolic compartment to be esterified, to regulate SREBP2 target genes, and ultimately, to be excreted in the feces. Presumably the pool of unesterified cholesterol in the lysosomes of normal mice was very small because of effective operation of the NPC1/NPC2 complex, so that sterol homeostasis in the tissues of these animals was unaffected by administration of CYCLO.

Second, if this interpretation is correct, it implies that CYCLO actually is taken up by the tissues, reaches the E/L compartment of cells throughout the body, and facilitates the movement of unesterified cholesterol across the limiting membrane of the lysosomes. Clearly, molecules such as LDL or CYCLO can reach the E/L compartment by two mechanisms, receptor-mediated and/or bulk-phase endocytosis. In some organs, like the liver and adrenal, LDL clearance is very high (250-500 μ L/hr/g) because LDL binds to the LDLR and is concentrated within the endocytic vesicles (13, 43). The cells of all tissues, however, take up LDL, even when interaction with the LDLR is blocked by methylation (44, 45) or when the LDLR is inactivated (13, 43). In the mouse, the clearance rate of such receptor-independent or bulk-phase endocytosis varies from about 1 to about 20 μ L/hr/g in various tissues of the body (13, 43). Nevertheless, when NPC1 is mutated, LDL-cholesterol taken up by either receptor-mediated or bulk-phase endocytosis reaches the E/L compartment and is sequestered (13). Other molecules present in the bulk-phase of the pericellular fluid such as sucrose, albumin, or, presumably, CYCLO, would also be taken up into cells through this process and reach the E/L compartment.

The concentration of this CYCLO molecule in the bulk-phase of the endocytic vesicles is determined largely by the sieving effect of the capillary membranes in a particular organ. In the liver sinusoids where the capillary membrane

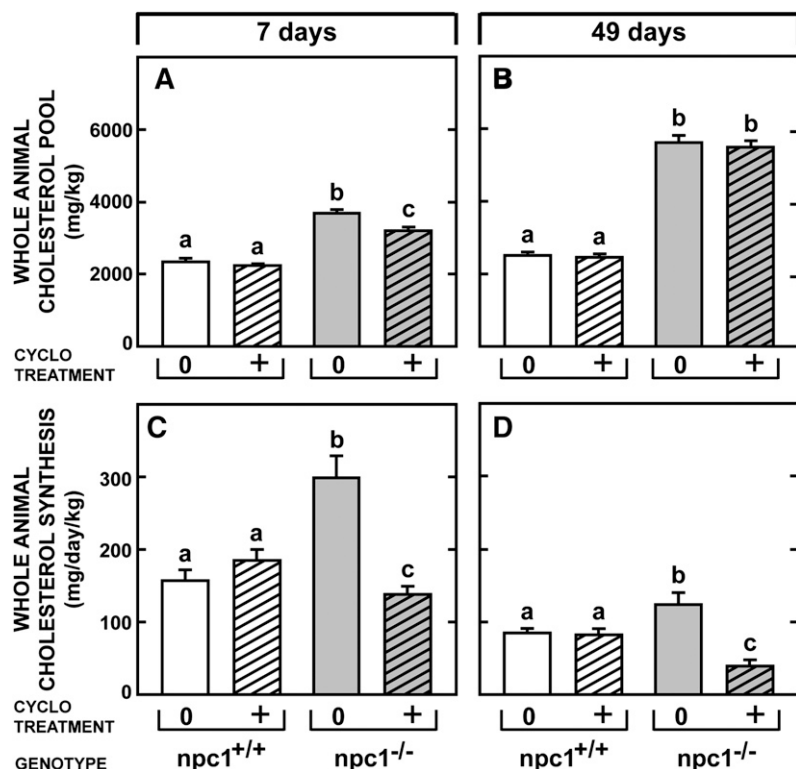


Fig. 6. Whole-animal cholesterol pools and synthesis rates in *npc1*^{+/+} and *npc1*^{-/-} mice given CYCLO at either 7 or 49 days of age. These animals were administered either saline or CYCLO at 7 or 49 days of age and then studied 24 h later. The whole-animal cholesterol pools were measured in the 8 groups of mice (A, B) as were the rates of whole-animal cholesterol synthesis (C, D). These values represent the mg of cholesterol per kg body weight and the mg of sterol synthesized per day per kg body weight, respectively. Each bar shows the mean \pm SEM for 6 animals, and significant differences are indicated by different letters. CYCLO, 2-hydroxypropyl- β -cyclodextrin ; NPC, Niemann-Pick type C.

is fenestrated, for example, the reflection coefficient for CYCLO is zero, and its concentration in the endocytic vesicles should equal its concentration in the plasma. The capillaries of other organs, and importantly, the capillaries of the CNS offer greater resistance to molecular diffusion so that the concentration of CYCLO in the pericellular fluid and endocytic vesicles may be less than the concentration in the plasma. Nevertheless, it is of interest that the concentration of CYCLO achieved in the plasma both in

the 7-day-old and 49-day-old mice was at the 1–3 mM level, a concentration range where CYCLO has been shown in vitro to act as an effective shuttle for moving cholesterol between cell membranes and lipoproteins (46). As it is likely that the concentration of CYCLO in the endocytic vesicles throughout the body was in the range of 0.1–3 mM, this ability to shuttle cholesterol through an aqueous phase may conceivably be the mechanism whereby this compound overcomes the transport defect in *npc1*^{-/-} mice.

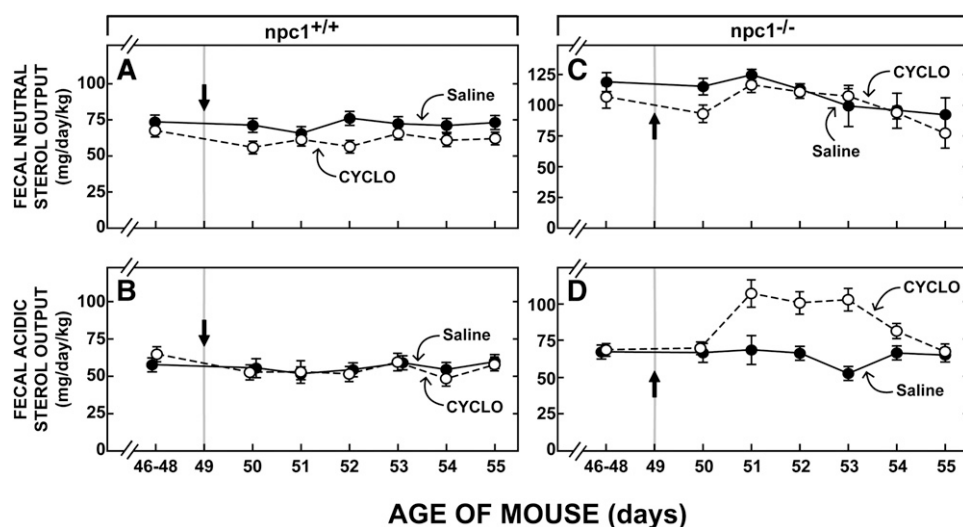


Fig. 7. Fecal neutral and acidic sterol output in *npc1*^{+/+} and *npc1*^{-/-} mice after administration of CYCLO. The first point in each panel represents the baseline level of sterol output measured over the 3 days (days 46–48) prior to administration of either saline or CYCLO to mice at 49 days of age (indicated by arrows). Feces were collected in daily aliquots over the next 6 days. The amount of neutral (A, C) and acidic (B, D) sterol in each sample was then determined. Each point represents the mean \pm SEM for 6 animals. CYCLO, 2-hydroxypropyl- β -cyclodextrin ; NPC, Niemann-Pick type C.

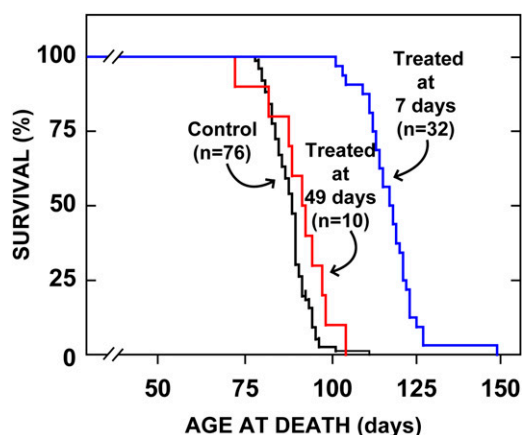


Fig. 8. Age at death of animals treated with CYCLO at either 7 or 49 days of age. Groups of *npcl*^{-/-} mice were administered a single injection of CYCLO (4,000 mg/kg) at either 7 days of age or 49 days of age, and were then allowed to live out their lives. The control animals received only saline injections. The lifespan of only the animals treated at 7 days of age was significantly ($P < 0.05$) prolonged. CYCLO, 2-hydroxypropyl- β -cyclodextrin.


Third, despite the marked difference in the duration of exposure to the tissues (Fig. 2), both the young and mature mice apparently responded equally well to administration of CYCLO. With the exception of the lungs, the liver, brain, and other organs all showed similar responses 24 h after CYCLO administration with a reduction in the concentration of unesterified cholesterol, an increase of cholesteryl esters, and downregulation of mRNAs encoding markers of macrophage infiltration and activation (Fig. 3–5). Furthermore, the relative changes in each of these parameters was similar in the 7- and 49-day-old mice, even in the brain (Fig. 4), suggesting that during this 24-h period both the young and mature *npcl*^{-/-} animals were equally sensitive to changing lysosomal permeability after exposure to CYCLO.

Fourth, however, these two groups of animals did respond quantitatively differently in terms of altering the whole-body burden of cholesterol after exposure to CYCLO. The whole-animal cholesterol pool decreased by 469 mg/kg 24 h after CYCLO administration to the 7-day-old *npcl*^{-/-} mice but by only 105 mg/kg in the mature animals. Furthermore, after the single dose of CYCLO, the whole-body pool of cholesterol ultimately declined by 910 mg/kg in the young mice (27) but by only 150 mg/kg in the 49-day-old animals (Fig. 7). Importantly, this 6-fold difference in ultimate response of the whole-animal cholesterol pool corresponded almost exactly to the 6-fold difference in exposure time of the tissues to circulating CYCLO in the 7-day-old and 49-day-old mice (Fig. 2). Again, this finding supported the conclusion that the organs of the young and mature animals, including the CNS, were equally sensitive to the administration of CYCLO. The lesser ultimate reduction in the whole-animal cholesterol pool seen in the 49-day-old mice probably only reflected the more rapid clearance of CYCLO and, therefore, the lesser exposure time in these mature animals.

Fifth, once the transport defect in the E/L compartments of cells had been overcome, the liberated unesterified cho-

lesterol in peripheral organs must necessarily have been transported to the liver where it, along with sterol released from hepatic lysosomes, could be excreted from the body as fecal sterols. Given the published observation that following CYCLO administration the mRNA level for the LXR target gene CYP7A1 was increased in the liver whereas those for ABCG5/8 were not (27), it was not surprising that the output of acidic, but not neutral, fecal sterols accounted for the reduction in the total-animal cholesterol pool (Fig. 7). Apparently, the times required for reversal of the transport defect and for the movement of this sequestered sterol through the various metabolic pathways for excretion were very different. The movement of unesterified cholesterol from the E/L compartment with the formation of cholesteryl esters and suppression of sterol synthesis could be detected within a few h of administration of the CYCLO. This excess sterol was then temporarily stored as esters in the peripheral organs, and these were only slowly hydrolyzed so the cholesterol could be moved to the liver through the HDL pathway. There the excess pool of cholesterol from these peripheral organs and from the liver was converted to bile acids, and ultimately, these were excreted through the enterohepatic circulation into the feces. Thus, following CYCLO administration, reversal of the transport defect in the E/L compartment was apparently very rapid, whereas movement of the released pool of cholesterol out of the body required several days.

CONCLUSION

While these studies demonstrated that CYCLO reversed the intracellular transport defect brought about by a mutation in the NPC1 protein in the young and mature animals, they raised several important questions that will require further investigation. First, would repetitive administration of CYCLO from birth fully normalize the cholesterol pools in every organ in the body and in the whole animal? Second, if so, would such treatment completely prevent clinical disease in the *npcl*^{-/-} mice or would organs like the lung and, particularly, the CNS still show progressive, although delayed, cell damage? Finally, is the concentration of CYCLO achieved in the pericellular fluid of the CNS adequately high to totally prevent neurodegeneration, or will direct introduction of this molecule into the brain be required? The answers to these important questions remain to be elucidated. 

The authors express their appreciation to Heather Waddell, S. Sean Campbell, Carolyn Smith, Stephen Ostermann and Monti Schneiderman for their excellent technical assistance, and to Annemarie Kelsey for expert preparation of the manuscript.

REFERENCES

1. Pentchev, P. G., M. T. Vanier, K. Suzuki, and M. C. Patterson. 1995. Niemann-Pick disease type C: a cellular cholesterol lipidosis. In *The Metabolic and Molecular Bases of Inherited Disease*. C. R. Scriver, A. L. Beaudet, W. S. Sly, D. Valle, J. B. Stanbury, J.

- B. Wyngaarden, and D. S. Fredrickson, editors. McGraw-Hill, New York. 2625–2639.
2. Patterson, M. C. 2003. A riddle wrapped in a mystery: understanding Niemann-Pick disease, type C. *Neurologist*. **9**: 301–310.
 3. Vanier, M. T., and G. Millat. 2003. Niemann-Pick disease type C. *Clin. Genet*. **64**: 269–281.
 4. Manabe, T., T. Yamane, Y. Higashi, P. G. Pentchev, and K. Suzuki. 1995. Ultrastructural changes in the lung in Niemann-Pick type C mouse. *Virchows Arch*. **427**: 77–83.
 5. Neufeld, E. B., M. Wastney, S. Patel, S. Suresh, A. M. Cooney, N. K. Dwyer, C. F. Roff, K. Ohno, J. A. Morris, E. D. Carstea, et al. 1999. The Niemann-Pick C1 protein resides in a vesicular compartment linked to retrograde transport of multiple lysosomal cargo. *J. Biol. Chem*. **274**: 9627–9635.
 6. Millat, G., K. Chikh, S. Naureckiene, D. E. Sleat, A. H. Fensom, K. Higaki, M. Elleder, P. Lobel, and M. T. Vanier. 2001. Niemann-Pick disease type C: spectrum of HE1 mutations and genotype/phenotype correlations in the NPC2 group. *Am. J. Hum. Genet*. **69**: 1013–1021.
 7. Loftus, S. K., J. A. Morris, E. D. Carstea, J. Z. Gu, C. Cummings, A. Brown, J. Ellison, K. Ohno, M. A. Rosenfeld, D. A. Tagle, et al. 1997. Murine model of Niemann-Pick C disease: mutation in a cholesterol homeostasis gene. *Science*. **277**: 232–235.
 8. Carstea, E. D., J. A. Morris, K. G. Coleman, S. K. Loftus, D. Zhang, C. Cummings, J. Gu, M. A. Rosenfeld, W. J. Pavan, D. B. Krizman, et al. 1997. Niemann-Pick C1 disease gene: homology to mediators of cholesterol homeostasis. *Science*. **277**: 228–231.
 9. Naureckiene, S., D. E. Sleat, H. Lackland, A. Fensom, M. T. Vanier, R. Wattiaux, M. Jadot, and P. Lobel. 2000. Identification of HE1 as the second gene of Niemann-Pick C disease. *Science*. **290**: 2298–2301.
 10. Xie, C., S. D. Turley, P. G. Pentchev, and J. M. Dietschy. 1999. Cholesterol balance and metabolism in mice with loss of function of Niemann-Pick C protein. *Am. J. Physiol*. **276**: E336–E344.
 11. Xie, C., D. K. Burns, S. D. Turley, and J. M. Dietschy. 2000. Cholesterol is sequestered in the brains of mice with Niemann-Pick type C disease but turnover is increased. *J. Neuropathol. Exp. Neurol*. **59**: 1106–1117.
 12. Zervas, M., K. Dobrenis, and S. U. Walkley. 2001. Neurons in Niemann-Pick disease type C accumulate gangliosides as well as unesterified cholesterol and undergo dendritic and axonal alterations. *J. Neuropathol. Exp. Neurol*. **60**: 49–64.
 13. Liu, B., C. Xie, J. A. Richardson, J. D. Horton, S. D. Turley, and J. M. Dietschy. 2007. Receptor-mediated and bulk-phase endocytosis cause macrophage and cholesterol accumulation in Niemann-Pick C disease. *J. Lipid Res*. **48**: 1710–1723.
 14. Beltroy, E. P., J. A. Richardson, J. D. Horton, S. D. Turley, and J. M. Dietschy. 2005. Cholesterol accumulation and liver cell death in mice with Niemann-Pick type C disease. *Hepatology*. **42**: 886–893.
 15. Li, H., J. J. Repa, M. A. Valasek, E. P. Beltroy, S. D. Turley, D. C. German, and J. M. Dietschy. 2005. Molecular, anatomical, and biochemical events associated with neurodegeneration in mice with Niemann-Pick type C disease. *J. Neuropathol. Exp. Neurol*. **64**: 323–333.
 16. Brown, M. S., and J. L. Goldstein. 1986. A receptor-mediated pathway for cholesterol homeostasis. *Science*. **232**: 34–47.
 17. Xie, C., S. D. Turley, and J. M. Dietschy. 2009. ABCA1 plays no role in the centripetal movement of cholesterol from peripheral tissues to the liver and intestine in the mouse. *J. Lipid Res*. **50**: 1316–1329.
 18. Quan, G., C. Xie, J. M. Dietschy, and S. D. Turley. 2003. Ontogenesis and regulation of cholesterol metabolism in the central nervous system of the mouse. *Dev. Brain Res*. **146**: 87–98.
 19. Turley, S. D., D. K. Burns, C. R. Rosenfeld, and J. M. Dietschy. 1996. Brain does not utilize low density lipoprotein-cholesterol during fetal and neonatal development in the sheep. *J. Lipid Res*. **37**: 1953–1961.
 20. Mauch, D. H., K. Nägler, S. Schumacher, C. Göritz, E.-C. Müller, A. Otto, and F. W. Pfrieger. 2001. CNS synaptogenesis promoted by glia-derived cholesterol. *Science*. **294**: 1354–1357.
 21. Pfrieger, F. W. 2003. Outsourcing in the brain: do neurons depend on cholesterol delivery by astrocytes? *Bioessays*. **25**: 72–78.
 22. Hayashi, H., R. B. Campenot, D. E. Vance, and J. E. Vance. 2004. Glial lipoproteins stimulate axon growth of central nervous system neurons in compartmented cultures. *J. Biol. Chem*. **279**: 14009–14015.
 23. Beltroy, E. P., B. Liu, J. M. Dietschy, and S. D. Turley. 2007. Lysosomal unesterified cholesterol content correlates with liver cell death in murine Niemann-Pick type C disease. *J. Lipid Res*. **48**: 869–881.
 24. Repa, J. J., H. Li, T. C. Frank-Cannon, M. A. Valasek, S. D. Turley, M. G. Tansey, and J. M. Dietschy. 2007. Liver X receptor activation enhances cholesterol loss from the brain, decreases neuroinflammation, and increases survival of the NPC1 mouse. *J. Neurosci*. **27**: 14470–14480.
 25. Griffin, L. D., W. Gong, L. Verot, and S. H. Mellon. 2004. Niemann-Pick type C disease involves disrupted neurosteroidogenesis and responds to allopregnanolone. *Nat. Med*. **10**: 704–711.
 26. Liu, B., H. Li, J. J. Repa, S. D. Turley, and J. M. Dietschy. 2008. Genetic variations and treatments that affect the lifespan of the NPC1 mouse. *J. Lipid Res*. **49**: 663–669.
 27. Liu, B., S. D. Turley, D. K. Burns, A. M. Miller, J. J. Repa, and J. M. Dietschy. 2009. Reversal of defective lysosomal transport in NPC disease ameliorates liver dysfunction and neurodegeneration in the npc1^{−/−} mouse. *Proc. Natl. Acad. Sci. USA*. **106**: 2377–2382.
 28. Christian, A. E., M. P. Haynes, M. C. Phillips, and G. H. Rothblat. 1997. Use of cyclodextrins for manipulating cellular cholesterol content. *J. Lipid Res*. **38**: 2264–2272.
 29. Yancey, P. G., W. V. Rodriguez, E. P. C. Kilsdonk, G. W. Stoudt, W. J. Johnson, M. C. Phillips, and G. H. Rothblat. 1996. Cellular cholesterol efflux mediated by cyclodextrins. *J. Biol. Chem*. **271**: 16026–16034.
 30. Irie, T., K. Fukunaga, M. K. Garwood, T. O. Carpenter, J. Pitha, and J. Pitha. 1992. Hydroxypropylcyclodextrins in parenteral use. II: effects on transport and disposition of lipids in rabbit and humans. *J. Pharm. Sci*. **81**: 524–528.
 31. Repa, J. J., and D. J. Mangelsdorf. 2000. The role of orphan nuclear receptors in the regulation of cholesterol homeostasis. *Annu. Rev. Cell Dev. Biol*. **16**: 459–481.
 32. Repa, J. J., and D. J. Mangelsdorf. 1999. Nuclear receptor regulation of cholesterol and bile acid metabolism. *Curr. Opin. Biotechnol*. **10**: 557–563.
 33. Sun, L.-P., J. Seemann, J. L. Goldstein, and M. S. Brown. 2007. Sterol-regulated transport of SREBPs from endoplasmic reticulum to Golgi: Insig renders sorting signal in Scap inaccessible to COPII proteins. *Proc. Natl. Acad. Sci. USA*. **104**: 6519–6526.
 34. Goldstein, J. L., R. A. DeBose-Boyd, and M. S. Brown. 2006. Protein sensors for membrane sterols. *Cell*. **124**: 35–46.
 35. Schwarz, M., D. W. Russell, J. M. Dietschy, and S. D. Turley. 1998. Marked reduction in bile acid synthesis in cholesterol 7 α -hydroxylase-deficient mice does not lead to diminished tissue cholesterol turnover or to hypercholesterolemia. *J. Lipid Res*. **39**: 1833–1843.
 36. Dietschy, J. M., and D. K. Spady. 1984. Measurement of rates of cholesterol synthesis using tritiated water. *J. Lipid Res*. **25**: 1469–1476.
 37. Turley, S. D., J. M. Andersen, and J. M. Dietschy. 1981. Rates of sterol synthesis and uptake in the major organs of the rat in vivo. *J. Lipid Res*. **22**: 551–569.
 38. Kurrasch, D. M., J. Huang, T. M. Wilkie, and J. J. Repa. 2004. Quantitative real-time polymerase chain reaction measurement of regulators of G-protein signaling mRNA levels in mouse tissues. *Methods Enzymol*. **389**: 3–15.
 39. Valasek, M. A., J. Weng, P. W. Shaul, R. G. W. Anderson, and J. J. Repa. 2005. Caveolin-1 is not required for murine intestinal cholesterol transport. *J. Biol. Chem*. **280**: 28103–28109.
 40. Schmittgen, T. D., and K. J. Livak. 2008. Analyzing real-time PCR data by the comparative CT method. *Nat. Protoc*. **3**: 1101–1108.
 41. Pitha, J., A. Gerloczy, and A. Olivi. 1994. Parenteral hydroxypropyl cyclodextrins: intravenous and intracerebral administration of lipophiles. *J. Pharm. Sci*. **83**: 833–837.
 42. Xie, C., S. D. Turley, and J. M. Dietschy. 2000. Centripetal cholesterol flow from the extrahepatic organs through the liver is normal in mice with mutated Niemann-Pick type C protein (NPC1). *J. Lipid Res*. **41**: 1278–1289.
 43. Osono, Y., L. A. Woollett, J. Herz, and J. M. Dietschy. 1995. Role of the low density lipoprotein receptor in the flux of cholesterol through the plasma and across the tissues of the mouse. *J. Clin. Invest*. **95**: 1124–1132.
 44. Spady, D. K., D. W. Bilheimer, and J. M. Dietschy. 1983. Rates of receptor-dependent and -independent low density lipoprotein uptake in the hamster. *Proc. Natl. Acad. Sci. USA*. **80**: 3499–3503.
 45. Spady, D. K., J. B. Meddings, and J. M. Dietschy. 1986. Kinetic constants for receptor-dependent and receptor-independent low density lipoprotein transport in the tissues of the rat and hamster. *J. Clin. Invest*. **77**: 1474–1481.
 46. Atger, V. M., M. de la Llera Moya, G. W. Stoudt, W. V. Rodriguez, M. C. Phillips, and G. H. Rothblat. 1997. Cyclodextrins as catalysts for the removal of cholesterol from macrophage foam cells. *J. Clin. Invest*. **99**: 773–780.